An Efficient Cobalt Catalyst for Ambient Temperature Nitrile Dihydroboration, the Elucidation of a Chelate-Assisted Borylation Mechanism, and a New Synthetic Route to Amides

Chandrani Ghosh,[†] Suyeon Kim,[‡,§] Matthew R. Mena,[†] Jun-Hyeong Kim,[‡,§] Raja Pal,[†] Christopher L. Rock,[†] Thomas L. Groy,[†] Mu-Hyun Baik, [‡,§,*] and Ryan J. Trovitch[†,*]

[†]School of Molecular Sciences, Arizona State University, Tempe, Arizona 85287, United States

[‡]Department of Chemistry, Korea Advanced Institute of Science and Technology (KAIST), Daejeon 34141, Republic of Korea

[§]Center for Catalytic Hydrocarbon Functionalizations, Institute for Basic Science (IBS), Daejeon 34141, Republic of Korea

ABSTRACT: *N*,*N*-Diborylamines have emerged as promising reagents in organic synthesis; however, their efficient preparation and full synthetic utility have yet to be realized. To address both shortcomings, an effective catalyst for nitrile dihydroboration was sought. Heating $CoCl_2$ in the presence of ^{PyEt}PDI afforded the six-coordinate Co(II) salt, [(^{PyEt}PDI)CoCl][Cl]. Upon adding 2 equivalents of $NaEt_3BH$, hydride transfer to one chelate imine functionality was observed, resulting in the formation of (κ^4-*N,N,N,N*-$^{PyEt}IP^{CHMe}N^{EtPy}$)Co. Single crystal X-ray diffraction and density functional theory calculations revealed that this compound possesses a low spin Co(II) ground state featuring antiferromagnetic coupling to a singly reduced imino(pyridine) moiety. Importantly, (κ^4-*N,N,N,N*-$^{PyEt}IP^{CHMe}N^{EtPy}$)Co was found to catalyze the dihydroboration of nitriles using HBPin with turnover frequencies of up to 380 h^{-1} at ambient temperature. Stoichiometric addition experiments revealed that HBPin adds across the Co–N_{amide} bond to generate a hydride intermediate that can react with additional HBPin or nitriles. Computational evaluation of the reaction coordinate revealed that the B–H addition and nitrile insertion steps occur on the antiferromagnetically coupled triplet spin manifold. Interestingly, formation of the borylimine intermediate was found to occur following BPin transfer from the borylated chelate arm to regenerate (κ^4-*N,N,N,N*-$^{PyEt}IP^{CHMe}N^{EtPy}$)Co. Borylimine reduction is in turn facile and follows the same ligand-assisted borylation pathway. The independent hydroboration of alkyl and aryl imines was also demonstrated at 25 °C. With a series of *N*,*N*-diborylamines in hand, their addition to carboxylic acids allowed for the direct synthesis of amides at 120 °C, without the need for exogenous coupling reagent.

INTRODUCTION

The reduction of nitriles is an attractive way to access amines that are ubiquitous in the pharmaceutical, agrochemical, and specialty chemical industries.[1] The direct hydrogenation of nitriles represents an atom efficient approach; however, this transformation can proceed with poor product selectivity, affording a mixture of primary and secondary amines.[2] Moreover, nitrile hydrogenation has largely relied on the utilization of precious metals[3] since Earth-abundant metal catalysts require elevated temperatures and H_2 pressures.[4] Nitrile reduction can also be achieved using stoichiometric amounts of $LiAlH_4$ or $LiBH_4$; however, the pyrophoric nature of these reagents makes this method less attractive.

The dihydroboration of nitriles represents an alternative nitrile reduction strategy that yields *N*,*N*-diborylamines (Figure 1, top), which are activated primary amine analogues. In 2012, Nikonov described a molybdenum-imido hydride complex, (2,6-^{i}Pr$_2$PhN)Mo(H)(Cl)(PMe_3)$_3$, that catalyzes benzonitrile and acetonitrile dihydroboration (5 mol %, 22 °C, 12 h, TOF = 1.7 h^{-1}).[5] The scope was ultimately expanded upon and the dihydride variant (2,6-^{i}Pr$_2$PhN)MoH_2(PMe_3)$_3$ was also found to mediate this transformation.[6] In 2015, the Szymczak group demonstrated that a proton-switchable, bifunctional Ru

compound catalyzes nitrile dihydroboration at 5 mol % loading (25–45 °C with maximum TOF of 60 h^{-1}).[7] Subsequently, Gunanathan and coworkers reported nitrile and imine hydroboration at 60 °C using [Ru(*p*-cymene)Cl_2]$_2$ (1.0 mol %, 60 °C, with TOF up to 6.7 h^{-1})[8] while the Hill[9] and Ma[10] groups described *β*-diketiminate magnesium catalysts that operate at the same temperature (TOF up to 20 h^{-1}). In 2017, Shimada and coworkers achieved nitrile dihydroboration with HBcat in the presence of nickel(II) bis(acetylacetonato) derivatives at room temperature (TOF = 11 h^{-1}).[11] Meanwhile, Nakazawa reported an iron-indium complex, [Fe(CH_3CN)$_6$][*cis*-Fe(CO)$_4$($InCl_3$)$_2$], which successfully converted both aromatic and aliphatic nitriles into their corresponding diborylamines in the presence of HBPin at 10 mol % catalyst loading at 80 °C (TOF = 0.4 h^{-1}).[12] Recent reports have demonstrated that nitrile dihydroboration can be catalyzed by Lewis acids including aluminium reagents[13] and lanthanide compounds.[14] Very recently, Tobita and coworkers reported modest nitrile dihydroboration activity using HBPin in the presence of bis(silyl)xanthene Ru catalysts.[15]

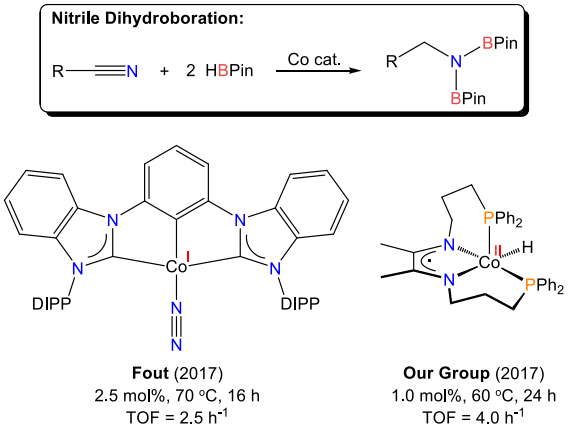

Figure 1. Diborylamines *via* Co-catalyzed nitrile dihydroboration.

Cobalt catalysts have been extensively utilized for hydride transfer reactions[16] including hydrogenation,[16a,16b,16l-o] hydrosilylation,[16e,16g,16h,17] and hydroboration[16i-k] of unsaturated substrates. Only recently has their utility been extended to nitrile dihydroboration. In 2017, Fout and co-workers showed that (^{DIPP}CCC)CoN_2 (DIPP = 2,6-diisopropylphenyl, Figure 1, left) catalyzes nitrile reduction in the presence of HBPin at 2.5 mol % loading at 70 °C.[18] Concurrently, our group described an α-diimine (DI) cobalt hydride catalyst, (^{Ph2PPr}DI)CoH (Figure 1, right), that catalyzes nitrile dihydroboration using HBPin at a slightly lower loading (1.0 mol %) and temperature (60 °C).[19] Considering that modest nitrile dihydroboration activity was noted for both (^{DIPP}CCC)CoN_2 and (^{Ph2PPr}DI)CoH, we sought to prepare a catalyst for this transformation that is efficient under ambient conditions. In the process of achieving this objective, we have revealed an unprecedented example of redox-active ligand-assisted borylation and a new synthetic application for *N*,*N*-diborylamines.

RESULTS AND DISCUSSION

Catalyst Synthesis and Characterization. Anticipating that strong phosphine coordination may hinder substrate activation by (^{Ph2PPr}DI)CoH, the pyridine-substituted pyridine diimine (PDI) chelate ^{PyEt}PDI was chosen for evaluation. This ligand was previously described[20] and its coordination to Mn led to the development of an efficient catalyst for carbonyl hydrosilylation.[21] To commence this study, ^{PyEt}PDI (1.05 eq.) was added to $CoCl_2$ and the mixture was heated to 95 °C in toluene. After 4 days,

complete consumption of $CoCl_2$ was observed, resulting in the formation of an insoluble light orange compound **1** (Eq. 1). ^{1}H NMR analysis revealed resonances over a 100 ppm range (Fig. S3) and magnetic susceptibility measurements using the Evans method yielded a value of 3.8 μ_B at ambient temperature. These data are consistent with a high-spin Co(II)-d^7 center in a pseudo-octahedral geometry exposing three unpaired electrons.[22] Density Functional Theory (DFT) calculations support this assignment and confirm that the high-spin configuration of **1** is 6.5 kcal/mol lower in energy than the low-spin analogue with only one unpaired electron on the cobalt center. Because PDI ligands can adopt a neutral, anionic, or dianionic state and become redox non-innocent, several possible electronic structure alternatives were considered. Most importantly, the Co(II)-center may formally donate an electron to the PDI ligand to adopt an electronic structure that is consistent with a Co(III)–(PDI^{-1}) system.[23] Despite significant efforts, we were unable to converge to such a state in our calculations and concluded that these non-classical states are not possible for **1**.

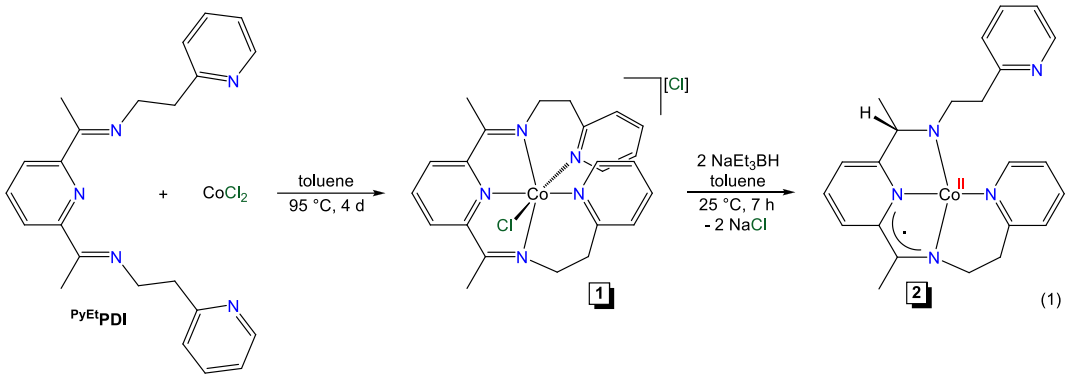

Recrystallization of **1** from chloroform at –35 °C afforded single crystals suitable for X-ray diffraction analysis, which confirmed a pseudo-octahedral coordination environment about Co and a square pyramidal ^{PyEt}PDI arrangement (Figure 2a). Even though the chelate ethylene bridges are fairly rigid, a nearly idealized N(4)–Co(1)–N(5) angle of 89.69(15)° is observed (See Table S2). In good agreement with the DFT results, the bond lengths of the PDI ligand in **1** are most consistent with a neutral PDI ligand[23] confirming our formal assignment of the (+II) oxidation state for the Co center.

In order to isolate a hydride complex similar to (^{Ph2PPr}DI)CoH,[19] **1** was treated with two equivalents of $NaEt_3BH$ in toluene, which afforded a forest green compound after stirring for 7 h at room temperature. The resulting product (**2**, Eq. 1) is diamagnetic based on multinuclear NMR spectroscopic analysis. In the ^{1}H NMR spectrum, two distinguishable resonances for the backbone methyl groups were detected; one doublet at 1.89 ppm and one upfield shifted singlet at –1.75 ppm. Accordingly, the existence of four unique ^{1}H NMR resonances for the chelate methylene groups suggested a lack of C_2 symmetry (Fig. S4). Although this compound was anticipated to have a hydride ligand, no hydride resonance was detected by ^{1}H NMR spectroscopy.

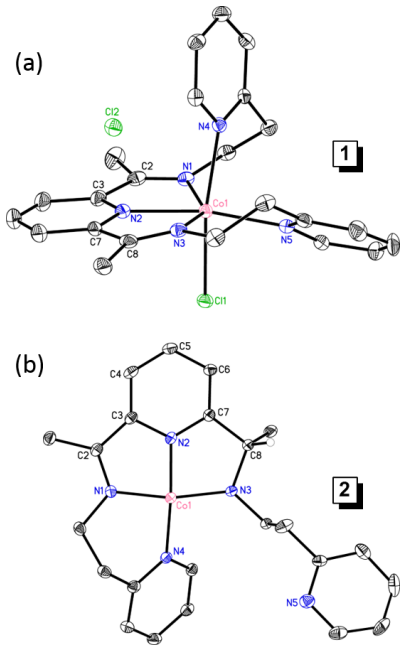

Figure 2. The solid-state structures of (a) **1** and (b) **2** at 30% probability ellipsoids. Hydrogen atoms and co-crystallized solvent molecules are omitted for clarity.

Table 1. Notable bond lengths (in Å) and bond angles (in °) for **1** and **2**.

	1 (Exp)	**1^{HS}(Calc)**	**1^{LS}(Calc)**	**2 (Exp)**	**2 (Calc)**
Co(1)–N(1)	2.173(4)	2.177	2.097	1.858(3)	1.886
Co(1)–N(2)	2.072(4)	2.107	1.865	1.825(3)	1.839
Co(1)–N(3)	2.155(4)	2.170	1.978	1.840(3)	1.851
Co(1)–N(4)	2.187(4)	2.236	2.356	1.914(2)	1.934
Co(1)–N(5)	2.149(4)	2.162	1.944	–	–
Co(1)–Cl(1)	2.4213(13)	2.368	2.406	–	–
N(1)–C(2)	1.271(7)	1.282	1.289	1.355(4)	1.352
C(2)–C(3)	1.489(8)	1.487	1.480	1.409(5)	1.421
C(3)–N(2)	1.348(7)	1.334	1.339	1.382(4)	1.369
N(2)–C(7)	1.331(7)	1.333	1.344	1.342(4)	1.333
C(7)–C(8)	1.483(8)	1.487	1.476	1.508(4)	1.504
C(8)–N(3)	1.284(7)	1.286	1.292	1.473(4)	1.462
N(1)–Co(1)–N(3)	147.36(16)	145.5	158.2	164.65(11)	165.7
N(2)–Co(1)–N(4)	99.37(16)	100.5	94.9	169.30(11)	171.5
N(2)–Co(1)–N(5)	162.37(17)	160.4	171.9	–	–
Cl(1)–Co(1)–N(4)	162.05(12)	162.3	170.5	–	–

Single crystals of **2** obtained from a concentrated ether/pentane solution at –35 °C were then analyzed by X-ray diffraction, which revealed κ^4-*N,N,N,N*-chelate coordination around Co with one uncoordinated pyridine arm (Figure 2b). Unexpectedly, hydride migration to an imine carbon atom took place (consistent with a C(8)-N(3) single bond distance of 1.473(4) Å), turning the formally neutral PDI chelate into an anionic imino(pyridal)amide ligand. The N(1)–C(2) and C(3)–N(2) distances of 1.355(4) and 1.382(4) Å are elongated and the C(2)–C(3) distance of 1.409 Å is contracted when compared

to neutral IP ligands (which exhibit distances of 1.28, 1.35, and 1.47 Å, respectively),[24] suggesting that the chelate of **2** is singly reduced. A contracted Co(1)–N(4) bond length of 1.914(2) Å is consistent with reported Co(II)–N_{amide} distances of Co(II) complexes,[25] and the bond angles of N(1)–Co(1)–N(2), N(1)–Co(1)–N(3), N(2)–Co(1)–N(3), and N(2)–Co(1)–N(4) were determined to be 82.11(11)°, 164.65(11)°, 84.12(11)°, and 169.30(11)°, respectively, giving rise to a distorted square planar geometry around the Co(II) center. DFT calculations show that singlet **2** (**^{1}2**), where the cobalt adopts a low-spin state and the unpaired electron is antiferromagnetically coupled to the ligand-based radical, is the lowest energy configuration with the putative triplet high-spin analogue (**^{3}2**) being 3.5 kcal/mol higher in energy, as illustrated in Figure 3. Notably, these spin states possess different coordination environments about cobalt. In **^{3}2**, the three t_2-like frontier orbitals are utilized to accommodate the three unpaired electrons. Moving to the energetically preferred low-spin **^{1}2**, first-order Jahn-Teller distortion demands a more square-planar geometry.[26]

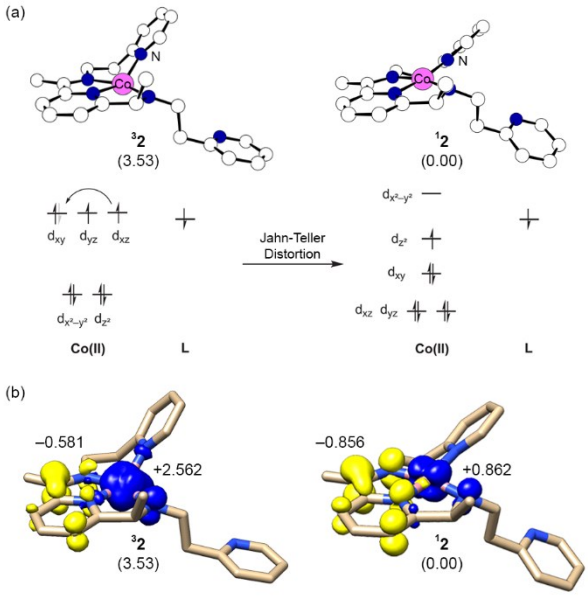

Figure 3. DFT-optimized geometries and corresponding (a) electronic structures and (b) Mulliken spin density (isovalue = 0.005) of **^{3}2** and **^{1}2**. Gibbs free energies are given in kcal/mol. Hydrogen atoms are omitted for clarity.

Nitrile Dihydroboration. Having isolated and characterized **2**, this precatalyst was tested for nitrile dihydroboration activity. In our previous study,[19] HBPin was found to be a suitable reductant for nitriles and a slight excess (2.2 eq.) was determined to enable complete conversion. Following these criteria, a benzene-d_6 solution of benzonitrile and HBPin was added to 1 mol % of **2**. The progress of the reaction was monitored by ^{1}H NMR spectroscopy, and remarkably, >99% conversion of the starting material to *N*,*N*-diborylamine was observed after 2 h at room temperature. Inspired by this result, 14 additional nitriles were tested (Table 2) and the respective *N*,*N*-diborylamine products were isolated *via* recrystallization from ether in modest yield. Precatalyst **2** was found to be efficient in reducing substituted benzonitriles that feature electron-donating (Entry ii and iii) and electron-withdrawing groups (Entry iv, v and vi) within the 2 h reaction time frame. The reduction of 4-fluorobenzonitrile and 4-(trifluoromethyl)benzonitrile (Entry v and vi) generated noticeable heat, suggesting that electron-withdrawing groups facilitate dihydroboration when compared to electron-donating groups and that there is a significant thermodynamic driving force for *N*,*N*-diborylamine formation. Precatalyst **2** was also determined to be tolerant of various functional groups including halides (Entry iv-vi), ethers (Entry iii, vii), and heterocycles (Entry viii). Aliphatic nitriles were also studied and it was found that acetonitrile reached complete conversion (Entry ix) while propionitrile and isobutyronitrile reached 74% and 52%

conversion (Entry x and xi), respectively, after 2 h at room temperature. However, amine and phosphine functionalities were found to hinder catalysis. 3-(Dimethylamino)propionitrile was determined to be only 43% converted to its corresponding diborylamine within 2 h and took 3 days for complete conversion, possibly due to substrate- and product-based NMe_2 coordination. At ambient temperature, 2-(diphenylphosphino)propionitrile did not undergo hydroboration, suggesting that phosphine coordination inhibits nitrile binding. Immediately upon adding a mixture of HBPin and 2-(diphenylphosphino)propionitrile to **2**, a color change from forest green to red was noticed, further substantiating this possibility. Heating this mixture to 60 °C allowed for the complete conversion of starting material within 2 h (Entry xiii); consistent with the fact that (^{Ph2PPr}DI)CoH-mediated dihydroboration requires heating to 60 °C.[19] Suspecting that **2** might be active for carbonyl hydroboration, 3.3 eq. of HBPin was added for the reduction of 4-acetylbenzonitrile, and after 2 h, it was found that both the acetyl and nitrile groups were reduced (Entry xiv). Conducting the dihydroboration of 4-methoxybenzonitrile in the dark did not reduce percent conversion under the same conditions, suggesting that light is not required for catalysis.

Table 2. Ambient temperature dihydroboration of nitriles using **2**.

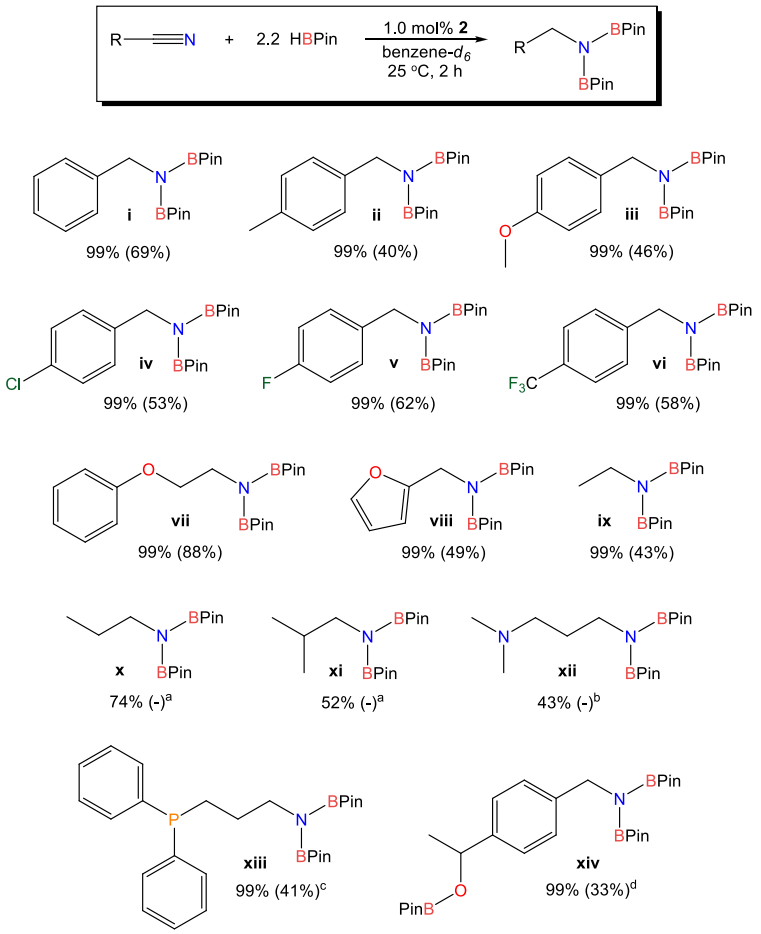

Isolated yields in parentheses. [a]Conversion at 2 h, complete conversion noted at 24 h. [b]Conversion at 2 h, complete conversion noted at 72 h. [c]Conversion after heating to 60 °C for 2 h. [d]3.3 equivalents of HBPin used.

To further define the utility of **2**, hydroboration experiments were conducted with a reduced catalyst loading under neat conditions. The dihydroboration of benzonitrile and 4-fluorobenzonitrile with 0.1 mol % **2** after 2 h in the absence of solvent showed 47% and 76% conversion, respectively, which equate to TOFs of 235 and 380 h^{-1}, respectively. A series of

control experiments were also conducted. Under the same conditions, the addition of 4-fluorobenzonitrile to HBPin in the absence of catalyst resulted in no detectable *N*,*N*-diborylamine after 2 h at ambient temperature. Given that magnesium,[9-10] aluminum,[13] and lanthanide[14] compounds have been shown to catalyze nitrile dihydroboration, we decided to screen several Lewis acid sources in the process of conducting control experiments. Although benzonitrile dihydroboration conversion was not observed using common Fe(II), Fe(III), Al(III), and La(III) sources, the addition of 10 mol % $BF_3{\cdot}Et_2O$ allowed for 10% conversion after 5 h at ambient temperature (Table S4). Surprisingly, 10 mol % $BH_3{\cdot}THF$, which is a common precursor for the preparation of HBPin, was found to catalyze benzonitrile dihydroboration to generate $PhCH_2N(BPin)_2$, with 24% conversion noted after 5 h at 25 °C (51% conversion after 5 h at 60 °C). Although catalyst **2** is significantly more active than BH_3, researchers evaluating the performance of catalysts for nitrile dihydroboration must pay special attention to the purity of their B–H source, especially if such trials are being heated.

Mechanism of Nitrile Dihydroboration. The mechanism of nitrile dihydroboration mediated by **2** was investigated using computational molecular modeling techniques augmented by a series of experiments. To obtain more information about the active form of the catalyst, one equivalent of 4-methoxybenzonitrile was added to a benzene-d_6 solution of **2**; however, no reaction was observed even after 24 h at room temperature based on ^{1}H NMR spectroscopy. Thus, **2** does not react directly with the nitrile substrate and requires an activation step, most likely involving a reaction with HBPin.

To test this hypothesis, one equivalent of HBPin was added to **2**. Although a transient color change was noticed, the solution immediately turned back to the catalyst color. The ^{1}H NMR spectrum of this mixture showed **2** as the major constituent along with new resonances for a second product. Adding a total of 2.2 equivalents of HBPin gave complete conversion to the newly formed product, as judged by ^{1}H NMR spectroscopy. Integration of the methyl resonances between 0.88–1.22 ppm accounted for 24 H (Fig. S7) and ^{13}C NMR spectroscopy showed the presence of two HBPin quaternary carbon environments at 82.25 and 83.22 ppm (Fig. S8). These spectroscopic observations suggest the formation of complex **3** (Eq. 2), which contains two pinacolborane functionalities, one of which is bound to the chelate amide nitrogen atom.

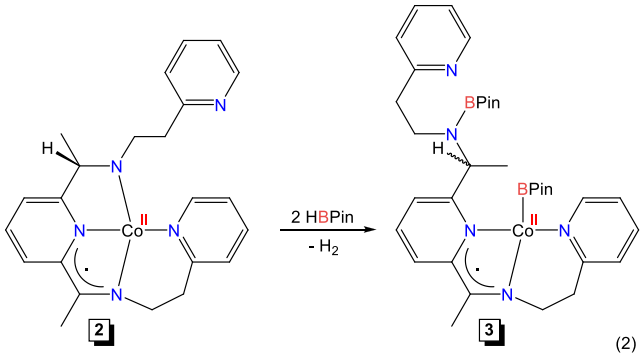

(2)

Interestingly, no reaction was observed upon addition of the nitrile substrate to **3**, indicating that this compound is a deactivation product. When one equivalent of HBPin was added to a 1:1 mixture of **2** and 4-methoxybenzonitrile, all HBPin was consumed and the *N*,*N*-diborylamine product was detected immediately along with unreacted nitrile as judged by ^{1}H NMR spectroscopy. Moreover, adding a second equivalent of HBPin to this mixture resulted in complete conversion of 4-methoxybenzonitrile to *N*,*N*-diborylamine. For $(^{DIPP}CCC)CoN_2$-catalyzed alkene and nitrile hydroboration,[18] the oxidative addition of borane to generate a metal hydride intermediate was proposed to be the catalyst activation step. In our case, a transient cobalt hydride is formed, but it quickly reacts with a second equivalent of HBPin or incoming nitrile, preventing its observation.

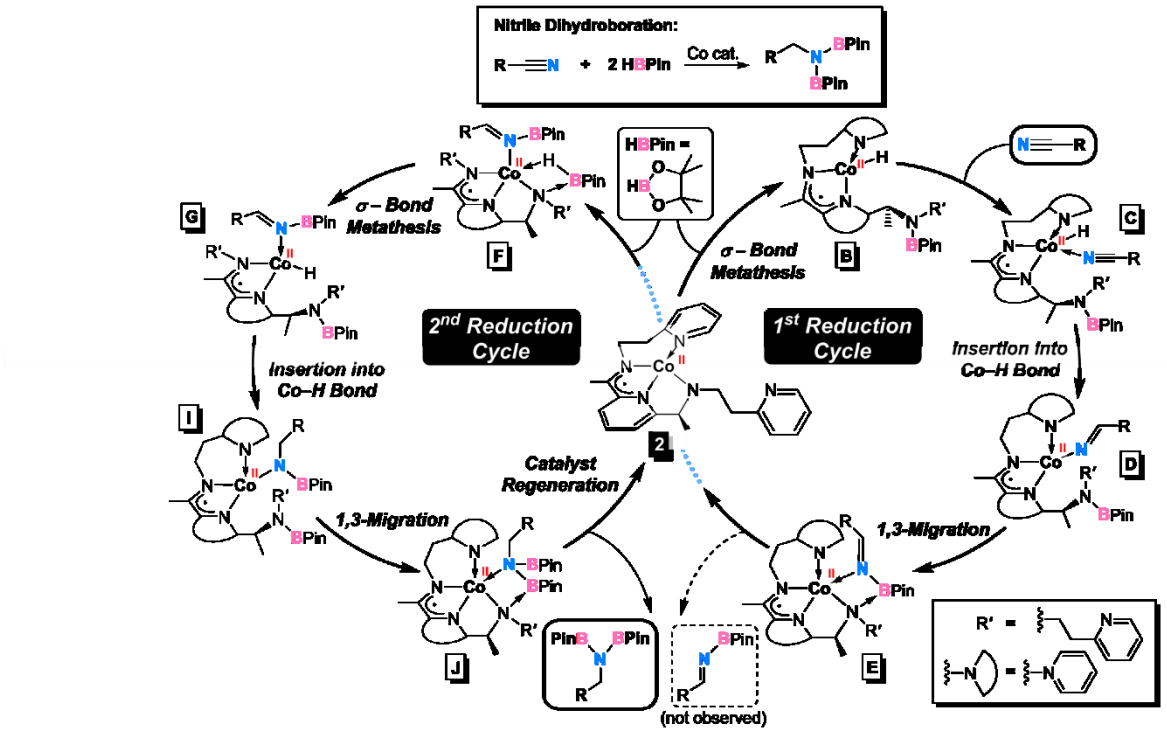

Figure 4. Catalytic cycle for **2**-catalyzed nitrile dihydroboration.

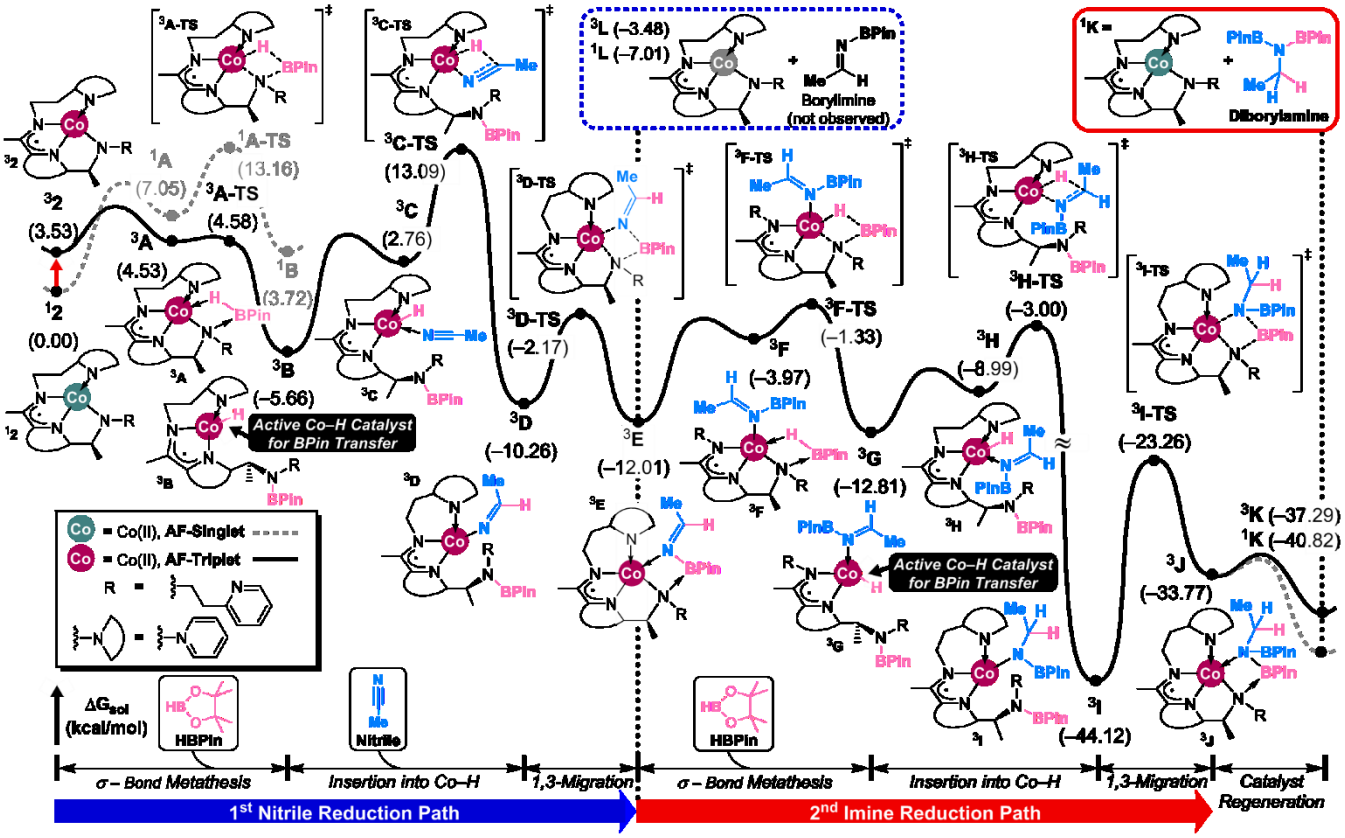

Figure 5. DFT-calculated energy profile of **2**-catalyzed acetonitrile dihydroboration involving antiferromagnetically coupled (AF) -singlet and -triplet spin states.

Figures 4 and 5 summarize the reaction mechanism obtained from our DFT calculations. Although the precatalyst ground state is an antiferromagnetically coupled singlet (^{1}**2**), as mentioned above, the triplet analogue ^{3}**2** is found to be much more reactive. Thus, we propose that the first step involves intersystem crossing into the triplet surface, where an equivalent of HBPin is first engaged to give the reactant complex ^{3}**A** featuring a four-membered Co–H–B–N metallacycle with an activated H–B bond. Metallacycles of this type have been reported, isolated, and crystallographically characterized during Mn-catalyzed carbon dioxide hydroboration.[27] In this case, ^{3}**A** is highly unstable, as σ–bond metathesis traversing the pseudo-transition state ^{3}**A-TS** to give the Co-hydride intermediate ^{3}**B** at –5.7 kcal/mol is barrierless. The same reaction requires 6.1 kcal/mol on the singlet surface, as shown in grey in Figure 5.

After the nitrile substrate, representatively modeled as acetonitrile in our calculations, binds to active catalyst ^{3}**B** to furnish intermediate ^{3}**C** at 2.8 kcal/mol, insertion into the Co–H bond occurs in an exergonic manner due to the formation of stable C–H bond. The overall barrier of insertion associated with the transition state ^{3}**C-TS** is the highest barrier of the first reduction cycle at 18.8 kcal/mol, which is consistent with a rapid reaction even at room temperature. To complete the first reduction cycle, the cobalt iminoamide complex ^{3}**D** undergoes ligand-assisted borylation, where the pendant ligand arm that temporarily carried the boryl group reattaches to the metal and initiates a 1,3-migration of the boryl group traversing the transition state ^{3}**D-TS** with a barrier of 8.1 kcal/mol to produce the corresponding borylimine intermediate product and regenerate the precatalyst in ^{3}**E**.

Formally, the borylimine intermediate product may detach from the precatalyst and be engaged by a second catalyst equivalent, as illustrated in the dashed blue box in Figure 5, but it is more convenient to assume that the borylimine remains coordinated and the second equivalent of HBPin is consumed to afford the reactant complex for the second reduction cycle. Our calculations indicate that this is an energetically viable scenario and the borylimine substrate remains firmly bound to the Co-center through the imino-nitrogen in the intermediate ^{3}**G**, which was located at –12.8 kcal/mol. Once it undergoes rearrangement which involves support from the ethylpyridine arm to form the analogous intermediate ^{3}**H**, subsequent insertion of the borylimine substrate into the Co–H bond can be readily facilitated traversing ^{3}**H-TS** as illustrated in Figure 6. This step is found to be highly exergonic with the insertion product ^{3}**I** being at –44.1 kcal/mol and the barrier being only 9.8 kcal/mol (^{3}**G** → ^{3}**H-TS**). The notably different insertion profiles in the first and second reduction cycles are easy to understand considering that imines have weaker C–N bonds than nitriles and are also easier to engage because of the imino-N lone pair. The ability of **2** to catalyze imine hydroboration at 25 °C has been verified, and several examples are provided in Table S5. Finally, ligand-assisted borylation takes place to regenerate **2** and produce the final product, $EtN(BPin)_2$. These energy profiles explain why it was impossible to observe borylimine intermediates by NMR spectroscopy during nitrile dihydroboration.

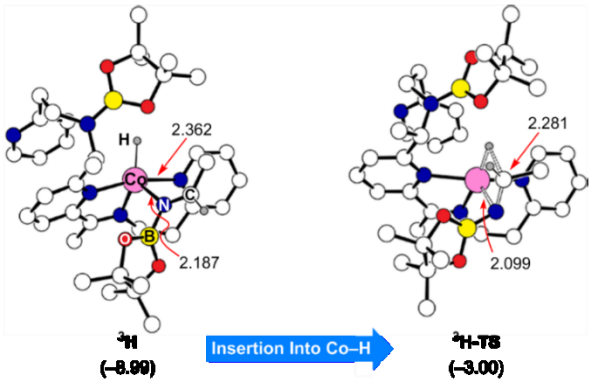

Figure 6. DFT-optimized geometries of ^{3}**H** and ^{3}**H-TS**. Only important hydrogen atoms are shown for clarity. Gibbs free energy and bond lengths are given in kcal/mol and Å, respectively.

The two reduction cycles leading to nitrile dihydroboration are summarized by several key steps, as illustrated in Figure 4. Reaction of **2** with one equivalent of HBPin produces a transient cobalt hydride intermediate (**B**) following B–H bond addition across the cobalt–amide bond. This reactive intermediate coordinates and inserts an incoming nitrile to generate the corresponding cobalt iminoamide complex (**D**). In order to utilize the borane equivalent being stored by the ligand, **D** can then undergo intramolecular 1,3-migration to release the corresponding borylimine (**E**). The consumption of a second equivalent of HBPin allows σ–bond metathesis to proceed and produces the cobalt hydride intermediate with the borylimine substrate bound to the cobalt-center (**G**). The borylimine moiety can subsequently insert into the cobalt–hydride bond to furnish the corresponding cobalt borylamido intermediate (**I**). Analogous transfer of BPin from the chelate to the amido ligand ultimately allows for *N*,*N*-diborylamine product release.

Utilization of Diborylamines for Amide Coupling. The reactivity of *N*,*N*-diborylamines remains understudied since primary amine derivatives of this type have only recently been prepared *via* hydroboration. In 2015, Nikonov and coworkers discovered that $PhCH_2N(BCat)_2$ reacts with benzaldehyde to produce the corresponding imine without the need for a dehydrating agent.[6] Borylamines can also serve as iminium generators, which can participate in nucleophilic addition reactions with enolates and cyanides.[28] Tobita and coworkers very recently reported that boryl- and diborylamines can be cross-coupled to aryl bromides in the presence of excess KO^{t}Bu and a catalytic quantity of $Pd(dba)_2$ and CyJohnPhos.[15]

Given that their applications remain limited, we have begun to evaluate the ability of *N*,*N*-diborylamines to act as amide-generating reagents. Upon heating a stoichiometric mixture of $PhCH_2N(BPin)_2$ and benzoic acid in benzene-d_6 to 120 °C in the absence of catalyst, complete conversion to *N*-benzylbenzamide and $O(BPin)_2$ was observed after 24 h. Recrystallizing this product mixture from benzene allowed for amide isolation in modest yield (Table 3, Entry i). Under the same conditions, four additional *N*,*N*-diborylamines from Table 2 were added to benzoic acid to prepare amides (Entry ii-v). We have also found that $PhCH_2N(BPin)_2$ undergoes direct coupling with 3-dimethylaminobenzoic acid and thiazole-4-carboxylic acid to prepare the respective *N*-benzyl amide (Entry vi-vii).

Table 3. Direct synthesis of *N*-substituted amides from carboxylic acid and the respective *N*,*N*-diborylamine.

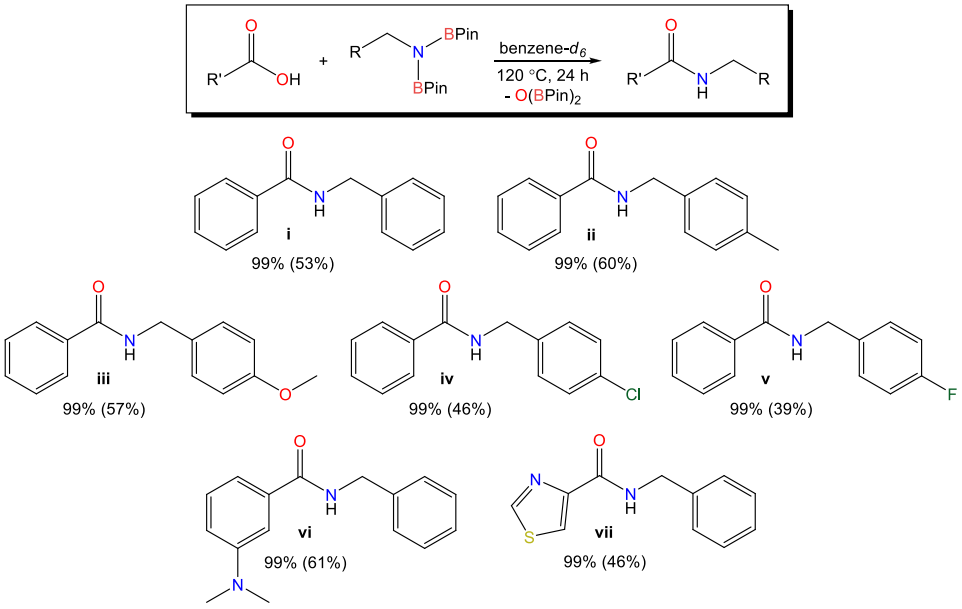

Percent conversion with isolated yields following benzene recrystallization in parentheses.

The examples in Table 3 represent the first reported uses of *N*,*N*-diborylamines as coupling partners to prepare *N*-substituted amides. While the substrate scope for this reaction is shown only as a proof of principle and is consequently limited, we expect that this methodology can be used to prepare a broad variety of amides, which are of widespread importance in biochemistry and the pharmaceutical industry. We hope to report the optimization, substrate scope, functional group tolerance, and mechanism of this transformation in a forthcoming contribution.[29]

CONCLUSIONS

Hydride transfer to ^{PyEt}PDI allowed for the preparation of **2**, which possesses a singlet ground state featuring a low-spin Co(II) center that is antiferromagnetically coupled to a ligand-based radical. This compound has been found to catalyze the dihydroboration of nitriles at ambient temperature with turnover frequencies of up to 380 h^{-1}, the highest reported for this transformation. While the catalyst was found to be tolerant of various functional groups, Lewis basic amine and phosphine substituents are believed to inhibit ambient temperature nitrile reduction due to competitive binding. Ultimately, a subset of the isolated *N*,*N*-diborylamine products were heated in the presence of a carboxylic acid to prepare the corresponding amides, a transformation that expands the known synthetic utility of such reagents. Detailed DFT calculations reveal that catalyst activation occurs *via* Co–N bond hydroboration and the entire catalytic cycle employes high-spin Co(II)-species, including the nitrile and borylimine insertion steps. Notably, elimination of the product is permitted by boryl group transfer from the ligand, allowing for concerted ligand redox and chemical non-innocence. Catalyst design strategies that bundle ligand-based electron storage with secondary sphere group transfer therefore represent a promising approach to enhance first-row metal catalyst efficiency, while lowering the required reaction temperature.

EXPERIMENTAL DETAILS

General Considerations: All reactions were performed inside an MBraun glovebox under an atmosphere of purified nitrogen. Toluene, tetrahydrofuran, pentane, and diethyl ether were purchased from Sigma-Aldrich, purified using a Pure Process Technology solvent system, and stored in the glove box over activated 4 Å molecular sieves and sodium before use. Benzene-d_6 and chloroform-*d* were purchased from Cambridge Isotope Laboratories and dried over 4 Å molecular sieves. 2,6-Diacetylpyridine, 2-(2-aminoethyl)pyridine, and benzonitrile were obtained from TCI America. 4-Methoxybenzonitrile, *p*-tolunitrile, 4-fluorobenzonitrile, 4-(trifluoromethyl)benzonitrile, 4-chlorobenzonitrile, 2-phenoxyacetonitrile, propionitrile, isobutyronitrile, benzoic acid, and 3-phenylpropanoic acid were obtained from Oakwood. Acetonitrile, 3-(dimethylamino)propionitrile, 4-acetylbenzonitrile, sodium triethylborohydride, pinacolborane, iodine, and 3-dimethylaminobenzoic acid were purchased from Sigma Aldrich. Cobalt dichloride was obtained from Strem while 2-furonitrile and thiazole-4-carboxylic acid were obtained from CombiBlocks. ^{PyEt}PDI[20] and 3-(diphenylphosphino)propionitrile[30] were synthesized according to literature procedures. Propionitrile and isobutyronitrile were dried over CaH_2 and distilled prior to use and all other liquid substrates were dried over 4 Å molecular sieves. 4-Fluorobenzonitrile was recrystallized from diethyl ether. Celite was purchased from Acros. The *N*,*N*-diborylamine products in Table 2 were isolated following recrystallization from diethyl ether under inert atmosphere since they decompose slowly in air.

Solution ^{1}H NMR spectra were recorded at room temperature (40 °C for **2**) on a Varian 400-MR (400 MHz) or Bruker Ascend 500 MHz NMR spectrometer. All ^{1}H NMR and ^{13}C NMR chemical shifts are reported in parts per million relative to $Si(CH_3)_4$ using internal $Si(CH_3)_4$ or ^{1}H (residual) and ^{13}C chemical shifts of the solvent as secondary standards. ^{19}F NMR spectra are

referenced to internal TMS through the proton channel. Elemental analyses were performed at Robertson Microlit Laboratories Inc. (Ledgewood, NJ). Solution state magnetic susceptibility was determined via the Evans method[31] on the Varian 400 MHz NMR spectrometer.

Preparation of [(^{PyEt}PDI)CoCl][Cl] (1): In a nitrogen filled glove box, a 100 mL thick-walled glass vessel was charged with $CoCl_2$ (1.166 g, 8.98 mmol) followed by ^{PyEt}PDI (3.50 g, 9.43 mmol) in approximately 30 mL of toluene. The apparatus was sealed, taken outside the box and heated at 95 °C in a pre-heated oil bath. After stirring for 4 days, the reaction mixture was filtered through Celite using chloroform and the solvent was removed under vacuum. The residual light brown solid was washed with pentane to remove unreacted ligand and then dried to yield 0.745 g (1.49 mmol, 17%) of a light brown solid identified as (^{PyEt}PDI)$CoCl_2$ (**1**). Single crystals of **1** as a pentachloroform solvate were obtained upon cooling a concentrated $CHCl_3$ solution to –35 °C. Anal. Calcd. for $C_{23}H_{25}N_5Cl_2Co \cdot 2(CHCl_3)$: C, 40.57%; H, 3.67%; N, 9.46%. Found: C, 40.88%; H, 3.79%; N, 9.46%. Magnetic susceptibility (Evans method in acetonitrile-d_3 solvent, 25 °C): μ_{eff} = 3.8 μ_B. ^{1}H NMR (chloroform-*d*, 25 °C): δ 91.41 (3233 Hz), 21.02 (49 Hz), 16.35 (1491 Hz), 15.02 (1491 Hz).

Preparation of (κ^4-*N*,*N*,*N*,*N*-^{PyEt}IP^{CHMe}N^{EtPy})Co (2): In a nitrogen filled glove box, a 100 mL round bottom flask was filled with **1** (99.9 mg, 0.1993 mmol) in approximately 20 mL of toluene and cooled in a liquid nitrogen cooled cold well for 20 min. A 20 mL scintillation vial containing a 1.0 M solution of $NaEt_3BH$ (0.4 mL, 0.3985 mmol) in toluene was also cooled in the cold well for 20 minutes. Then, the $NaEt_3BH$ was added dropwise to the round bottom flask containing the suspension of **1** in toluene. Initially, the color changed from light green to red and then to forest green color. After stirring for 7 h, the reaction mixture was filtered through Celite to remove the NaCl byproduct and then the solvent was removed under vacuum. The residue was washed with twice with pentane (3 mL each time) and then dried to obtain 64.5 mg (0.150 mmol, 75%) of a forest green solid identified as **2**. Single crystals were obtained by cooling a concentrated ether/pentane solution at –35 °C. Anal. Calcd for $C_{23}H_{26}N_5Co$: C, 64.03%; H, 6.07%; N, 16.23%. Found: C, 63.62%; H, 6.28%; N, 15.86%. ^{1}H NMR (500 MHz, toluene-d_8, 40 °C): 9.20 (d, *J* = 6.4 Hz, 1H, *pyridyl*), 8.66 (br, 1H, *pyridyl*), 7.75 (m, 1H, *pyridyl*), 7.71 (d, *J* = 8.2 Hz, 1H, *pyridyl*), 7.62 (t, *J* = 7.5 Hz, 1H, *pyridyl*), 7.28 (t, *J* = 6.3 Hz, 1H, *pyridyl*), 6.91 (m, 2H, *pyridyl*), 6.58 (d, *J* = 7.6 Hz, 1H, *pyridyl*), 6.54 (m, 1H, *pyridyl*), 6.30 (m, 1H, *pyridyl*), 6.25 (m, 1H, –C*H*), 3.82 (br, 1H, –CH_2), 3.55 (br, 1H, –CH_2), 3.25 (br, 1H, –CH_2), 2.95 (br, 1H, –CH_2), 2.81 (br, 1H. –CH_2), 2.33 (br, 1H, –CH_2), 1.93 (d, J = 6.4 Hz, 3H, –CH_3), 1.71 (br, 1H, –CH_2), -1.78 (s, 3H, –CH_3). ^{13}C NMR (126 MHz, toluene-d_8, 40 °C): 178.71 (*C*=N), 162.43 (*pyridyl*), 161.96 (*pyridyl*), 153.30 (*pyridyl*), 152.00 (*pyridyl*), 137.66 (*pyridyl*), 133.98 (*pyridyl*), 133.73 (*pyridyl*), 132.00 (*pyridyl*), 128.78 (*pyridyl*), 122.76 (*pyridyl*), 122.66 (*pyridyl*), 122.38 (*pyridyl*), 120.00 (*pyridyl*), 114.42 (*pyridyl*), 102.60 (*pyridyl*), 72.47 (–*C*H), 49.76 (–*C*H_2), 48.64 (–*C*H_2), 46.81 (–*C*H_2), 37.68 (–*C*H_2), 24.15 (–*C*H_3), 20.20 (–*C*H_3).

Preparation of (κ^3-*N*,*N*,*N*-^{PyEt}IP$^{CHMeN(BPin)EtPy}$)Co(BPin) (3): In a nitrogen filled glove box, a 20 mL scintillation vial was filled with **2** (19.9 mg, 0.0461 mmol) in approximately 10 mL of diethyl ether and stirred. To this stirred solution, 14.7 µL (0.1015 mmol) of pinacolborane was added. Immediately, a color change was observed from forest green to dark brown. After stirring for 24 h, the reaction mixture was filtered through Celite and then the solvent was removed under vacuum. The residue was washed twice with pentane (3 mL each time) and then dried to obtain 28.5 mg (0.042 mmol, 90%) of dark brown solid identified as **3**. Anal. Calcd for $C_{35}H_{50}B_2N_5O_4Co$: C, 61.34%; H, 7.35%; N, 10.22%. Found: C, 59.55%; H, 8.03%; N, 8.45%. ^{1}H NMR (400 MHz, toluene-d_8): 8.40 (br, 1H, *phenyl*), 7.23 (br, 3H, *phenyl*), 7.10 (m, 3H, *phenyl*), 6.81 (m, 2H, *phenyl*), 6.59 (m, 2H, *phenyl*), 4.82 (m, 1H, –C*H*), 3.53 (br, 2H, –CH_2), 3.03 (m, 2H, –CH_2), 2.12 (s, 3H, –CH_3), 1.77 (d, J = 5.4 Hz, 3H, –CH_3), 0.86-1.22 (s, 24H, –C(CH_3)$_2$), one –CH_2 not detected. ^{13}C NMR (126 MHz, toluene-d_8): 163.81 (*imine*), 161.54 (*pyridyl*),

149.84 (*pyridyl*), 135.66 (*pyridyl*), 123.58 (*pyridyl*), 121.04 (*pyridyl*), 119.75 (*pyridyl*), 83.22 (O*C*(CH_3)$_2$), 82.25 (O*C*(CH_3)$_2$), 57.88 (–*C*H), 45.92 (–*C*H_2), 41.60 (–*C*H_2), 41.44 (–*C*H_2), 25.01 (–*C*H_3), 20.81 (–*C*H_3), 15.92 (–*C*H_3).

Computational Details: All calculations were carried out using DFT[32] as implemented in the Jaguar 9.1 suite[33] of *ab initio* quantum chemistry programs. Geometry optimizations were performed with M06[34] functional and the 6-31G** basis set for main group atoms. Co was represented using the Los Alamos LACVP basis.[35] The energies of the optimized structures were reevaluated by additional single point calculations on each optimized geometry using Dunning's correlation consistent triple-ζ basis set cc-pVTZ(-f)[36] that includes a double set of polarization functions. For Co, we used a modified version of LACVP, designated as LACV3P, in which the exponents were decontracted to match the effective core potential with triple-ζ quality. Solvation energies were evaluated by a self-consistent reaction field (SCRF) approach based on accurate numerical solutions of the Poisson-Boltzmann equation. In the results reported, solvation calculations were carried out with the 6-31G**/LACVP basis at the optimized gas-phase geometry employing the dielectric constants of ε = 2.284 for benzene and 2.379 for toluene. As is the case for all continuum models, the solvation energies are subject to empirical parametrization of the atomic radii that are used to generate the solute surface. We employed the standard set of optimized radii in Jaguar for H (1.150 Å), B (2.042 Å), C(1.900 Å), N(1.600 Å), O(1.600 Å) and Co(1.436 Å).[37] Analytical vibrational frequencies within the harmonic approximation were computed with the 6-31G**/LACVP basis to confirm proper convergence to well-defined minima or saddle points on the potential energy surface.

The energy components have been computed with the following protocol. The free energy in solution phase G(sol) has been calculated as follows:

$$G(sol) = G(gas) + G^{solv} \quad (3)$$

$$G(gas) = H(gas) - TS(gas) \quad (4)$$

$$H(gas) = E(SCF) + ZPE \quad (5)$$

$$\Delta E(SCF) = \Sigma E(SCF) \text{ for products} - \Sigma E(SCF) \text{ for reactants} \quad (6)$$

$$\Delta G(sol) = \Sigma G(sol) \text{ for products} - \Sigma G(sol) \text{ for reactants} \quad (7)$$

ASSOCIATED CONTENT

The Supporting Information is available free of charge on the ACS Publications website at DOI:

Detailed hydroboration procedures, NMR spectroscopic data, crystallographic information for **1** (CCDC - 1922371) and **2** (CCDC - 1922372), and Cartesian coordinates of the DFT-optimized structures.

AUTHOR INFORMATION

Corresponding Author

*mbaik2805@kaist.ac.kr

*ryan.trovitch@asu.edu

ORCID

Suyeon Kim: 0000-0002-7032-1147

Jun-Hyeong Kim: 0000-0001-7747-5475

Mu-Hyun Baik: 0000-0002-8832-8187

Ryan J. Trovitch: 0000-0003-4935-6780

Notes

The authors declare no competing financial interests.

ACKNOWLEDGMENT

We thank the Institute for Basic Science (IBS-R10-A1) in Korea for financial support. This material is based upon work supported by the National Science Foundation under Grant No. 1651686.

REFERENCES

1. (a) Vries, J. G. d., *The handbook of homogeneous hydrogenation*. Wiley-Vch: 2007; (b) Oro, L. A.; Carmona, D.; Fraile, J. M., Hydrogenation Reactions. In *Metal-catalysis in Industrial Organic Processes*, 2006; pp 79–113.
2. Gomez, S.; Peters, J. A.; Maschmeyer, T., The Reductive Amination of Aldehydes and Ketones and the Hydrogenation of Nitriles: Mechanistic Aspects and Selectivity Control. *Adv. Synth. Catal.* **2002**, *344*, 1037–1057.
3. (a) Gunanathan, C.; Hölscher, M.; Leitner, W., Reduction of Nitriles to Amines with H_2 Catalyzed by Nonclassical Ruthenium Hydrides – Water-Promoted Selectivity for Primary Amines and Mechanistic Investigations. *Eur. J. Inorg. Chem.* **2011**, *2011*, 3381–3386; (b) Li, T.; Bergner, I.; Haque, F. N.; Zimmer-De Iuliis, M.; Song, D.; Morris, R. H., Hydrogenation of Benzonitrile to Benzylamine Catalyzed by Ruthenium Hydride Complexes with P−NH−NH−P Tetradentate Ligands: Evidence for a Hydridic−Protonic Outer Sphere Mechanism. *Organometallics* **2007**, *26*, 5940−5949; (c) Reguillo, R.; Grellier, M.; Vautravers, N.; Vendier, L.; Sabo-Etienne, S., Ruthenium-Catalyzed Hydrogenation of Nitriles: Insights into the Mechanism. *J. Am. Chem. Soc.* **2010**, *132*, 7854−7855; (d) Rajesh, K.; Dudle, B.; Blacque, O.; Berke, H., Homogeneous Hydrogenations of Nitriles Catalyzed by Rhenium Complexes. *Adv. Synth. Catal.* **2011**, *353*, 1479−1484; (e) Yoshida, T.; Okano, T.; Otsuka, S., Catalytic Hydrogenation of Nitriles and Dehydrogenation of Amines with the Rhodium(I) Hydrido Compounds $[RhH(PPr^i_3)_3]$ and $[Rh_2H_2(\mu\text{-}N_2)\{P(cyclohexyl)_3\}_4]$. *J. Chem. Soc. Chem. Commun.* **1979**, 870−871; (f) Chin, C. S.; Lee, B., Hydrogenation of Nitriles with Iridium-Triphenylphosphine Complexes. *Catal. Letters* **1992**, *14*, 135−140.
4. (a) Lange, S.; Elangovan, S.; Cordes, C.; Spannenberg, A.; Jiao, H.; Junge, H.; Bachmann, S.; Scalone, M.; Topf, C.; Junge, K.; Beller, M., Selective Catalytic Hydrogenation of Nitriles to Primary Amines Using Iron Pincer Complexes. *Catal. Sci. Technol.* **2016**, *6*, 4768−4772; (b) Mukherjee, A.; Srimani, D.; Chakraborty, S.; Ben-David, Y.; Milstein, D., Selective Hydrogenation of Nitriles to Primary Amines Catalyzed by a Cobalt Pincer Complex. *J. Am. Chem. Soc.* **2015**, *137*, 8888−8891; (c) Chakraborty, S.; Leitus, G.; Milstein, D., Selective Hydrogenation of Nitriles to Primary Amines Catalyzed by a Novel Iron Complex. *Chem. Commun.* **2016**, *52*, 1812−1815. (d) Bornschein, C.; Werkmeister, S.; Wendt, B.; Jiao, H.; Alberico, E.; Baumann, W.; Junge, H.; Junge, K.; Beller, M. Mild and selective hydrogenation of aromatic and aliphatic (di)nitriles with a well-defined iron pincer complex. *Nat. Commun.* **2014**, *5*, 4111. (e) Elangovan, S.; Topf, C.; Fischer, S.; Jiao, H.; Spannenberg, A.; Baumann, W.; Ludwig, R.; Junge, K.; Beller, M. Selective Catalytic Hydrogenations of Nitriles, Ketones, and Aldehydes by Well-Defined Manganese Pincer Complexes. *J. Am. Chem. Soc.* **2016**, *138*, 8809-8814. (f) Tokmic, K.; Jackson, B. J.; Salazar, A.; Woods, T. J.; Fout, A. R. Cobalt-Catalyzed and Lewis Acid-Assisted Nitrile Hydrogenation to Primary Amines: A Combined Effort. *J. Am. Chem. Soc.* **2017**, *139*, 13554-13561. (g) Adam, R.; Bheeter, C. B.; Cabrero-Antonino, J. R.; Junge, K.; Jackstell, R.; Beller, M. Selective Hydrogenation of Nitriles to Primary Amines by using a Cobalt Phosphine Catalyst. *ChemSusChem* **2017**, *10*, 842-846.
5. Khalimon, A. Y.; Farha, P.; Kuzmina, L. G.; Nikonov, G. I., Catalytic Hydroboration by an Imido-Hydrido Complex of Mo(IV). *Chem. Commun.* **2012**, *48*, 455−457.
6. Khalimon, A. Y.; Farha, P. M.; Nikonov, G. I., Imido–Hydrido Complexes of Mo(IV): Catalysis and Mechanistic Aspects of Hydroboration Reactions. *Dalton Trans.* **2015**, *44*, 18945−18956.
7. Geri, J. B.; Szymczak, N. K., A Proton-Switchable Bifunctional Ruthenium Complex That Catalyzes Nitrile Hydroboration. *J. Am. Chem. Soc.* **2015**, *137*, 12808−12814.
8. Kaithal, A.; Chatterjee, B.; Gunanathan, C., Ruthenium-Catalyzed Selective Hydroboration of Nitriles and Imines. *J. Org. Chem.* **2016**, *81*, 11153-11161.
9. Weetman, C.; Anker, M. D.; Arrowsmith, M.; Hill, M. S.; Kociok-Köhn, G.; Liptrot, D. J.; Mahon, M. F., Magnesium-Catalysed Nitrile Hydroboration. *Chem. Sci.* **2016**, *7*, 628−641.
10. Li, J.; Luo, M.; Sheng, X.; Hua, H.; Yao, W.; Pullarkat, S. A.; Xu, L.; Ma, M., Unsymmetrical β-Diketiminate Magnesium(I) Complexes: Syntheses and Application in Catalytic Hydroboration of Alkyne, Nitrile and Carbonyl Compounds. *Org. Chem. Front.* **2018**, *5*, 3538−3547.
11. Nakamura, G.; Nakajima, Y.; Matsumoto, K.; Srinivas, V.; Shimada, S., Nitrile Hydroboration Reactions Catalysed by Simple Nickel Salts, Bis(acetylacetonato)nickel(II) and Its Derivatives. *Catal. Sci. Technol.* **2017**, *7*, 3196−3199.

12. Ito, M.; Itazaki, M.; Nakazawa, H., Selective Double Hydroboration and Dihydroborylsilylation of Organonitriles by an Iron-indium Cooperative Catalytic System. *Inorg. Chem.* **2017**, *56*, 13709−13714.
13. (a) Bismuto, A.; Cowley, M. J.; Thomas, S. P., Aluminum-Catalyzed Hydroboration of Alkenes. *ACS Catal.* **2018**, *8*, 2001−2005; (b) Harinath, A.; Bhattacharjee, J.; Panda, T. K., Catalytic Hydroboration of Organic Nitriles Promoted by Aluminum Complex. *Adv. Synth. Catal.* **2019**, *361*, 850−857.
14. Huang, Z.; Wang, S.; Zhu, X.; Yuan, Q.; Wei, Y.; Zhou, S.; Mu, X., Well-Defined Amidate-Functionalized N-Heterocyclic Carbene-Supported Rare-Earth Metal Complexes as Catalysts for Efficient Hydroboration of Unactivated Imines and Nitriles. *Inorg. Chem.* **2018**, *57*, 15069−15078.
15. Kitano, T.; Komuro, T.; Tobita, H., Double and Single Hydroboration of Nitriles Catalyzed by a Ruthenium–Bis(silyl)xanthene Complex: Application to One-Pot Synthesis of Diarylamines and N-Arylimines. *Organometallics* **2019**, *38*, 1417−1420.
16. (a) Yuwen, J.; Chakraborty, S.; Brennessel, W. W.; Jones, W. D., Additive-Free Cobalt-Catalyzed Hydrogenation of Esters to Alcohols. *ACS Catal.* **2017**, *7*, 3735−3740; (b) Adam, R.; Cabrero-Antonino, J. R.; Spannenberg, A.; Junge, K.; Jackstell, R.; Beller, M., A General and Highly Selective Cobalt-Catalyzed Hydrogenation of N-Heteroarenes under Mild Reaction Conditions. *Angew. Chem. Int. Ed.* **2017**, *56*, 3216−3220; (c) Friedfeld, M. R.; Shevlin, M.; Hoyt, J. M.; Krska, S. W.; Tudge, M. T.; Chirik, P. J., Cobalt Precursors for High-Throughput Discovery of Base Metal Asymmetric Alkene Hydrogenation Catalysts. *Science* **2013**, *342*, 1076−1080; (d) Chen, C.; Huang, Y.; Zhang, Z.; Dong, X.-Q.; Zhang, X., Cobalt-Catalyzed (Z)-Selective Semihydrogenation of Alkynes with Molecular Hydrogen. *Chem. Commun.* **2017**, *53*, 4612−4615; (e) Chen, C.; Hecht, M. B.; Kavara, A.; Brennessel, W. W.; Mercado, B. Q.; Weix, D. J.; Holland, P. L., Rapid, Regioconvergent, Solvent-Free Alkene Hydrosilylation with a Cobalt Catalyst. *J. Am. Chem. Soc.* **2015**, *137*, 13244−13247; (f) Chen, C.; Dugan, T. R.; Brennessel, W. W.; Weix, D. J.; Holland, P. L., Z-Selective Alkene Isomerization by High-Spin Cobalt(II) Complexes. *J. Am. Chem. Soc.* **2014**, *136*, 945−955; (g) Teo, W. J.; Wang, C.; Tan, Y. W.; Ge, S., Cobalt-Catalyzed Z-Selective Hydrosilylation of Terminal Alkynes. *Angew. Chem. Int. Ed.* **2017**, *56*, 4328−4332; (h) Raya, B.; Biswas, S.; RajanBabu, T. V., Selective Cobalt-Catalyzed Reduction of Terminal Alkenes and Alkynes Using $(EtO)_2Si(Me)H$ as a Stoichiometric Reductant. *ACS Catal.* **2016,** *6*, 6318−6323; (i) Zhang, L.; Zuo, Z.; Leng, X.; Huang, Z., A Cobalt-Catalyzed Alkene Hydroboration with Pinacolborane. *Angew. Chem. Int. Ed.* **2014,** *53*, 2696−2700; (j) Zhang, L.; Zuo, Z.; Wan, X.; Huang, Z., Cobalt-Catalyzed Enantioselective Hydroboration of 1,1-Disubstituted Aryl Alkenes. *J. Am. Chem. Soc.* **2014**, *136*, 15501−15504; (k) Guo, J.; Cheng, B.; Shen, X.; Lu, Z., Cobalt-Catalyzed Asymmetric Sequential Hydroboration/Hydrogenation of Internal Alkynes. *J. Am. Chem. Soc.* **2017**, *139*, 15316−15319. (l) Friedfeld, M. R.; Shevlin, M.; Margulieux, G. W.; Campeau, L.-C.; Chirik, P. J. Cobalt-Catalyzed Enantioselective Hydrogenation of Minimally Functionalized Alkenes: Isotopic Labeling Provides Insight into the Origin of Stereoselectivity and Alkene Insertion Preferences. *J. Am. Chem. Soc.* **2016**, *138*, 3314-3324. (m) Tokmic, K.; Markus, C. R.; Zhu, L.; Fout, A. R. Well-Defined Cobalt(I) Dihydrogen Catalyst: Ecperimental Evidence for a Co(I)/Co(III) Redox Process in Olefin Hydrogenation. *J. Am. Chem. Soc.* **2016**, *138*, 11907-11913. (n) Tokmic, K.; Fout, A. R. Alkyne Semihydrogenation with a Well-Defined Nonclassical Co-H_2 Catalyst: A H_2 Spin on Isomerization and *E*-Selectivity. *J. Am. Chem. Soc.* **2016**, *138*, 13700-13705. (o) Tokmic, K.; Greer, R. B.; Zhu, L.; Fout, A. R. ^{13}C NMR Signal Enhancement Using Parahydrogen-Induced Polarization Mediated by a Cobalt Hydrogenation Catalyst. *J. Am. Chem. Soc.* **2018**, *140*, 14844-14850.
17. The dihydrosilylation of nitriles using a cobalt catalyst has recently been reported in Sanagawa, A.; Nagashima, H., Hydrosilane Reduction of Nitriles to Primary Amines by Cobalt–Isocyanide Catalysts. *Org. Lett.* **2019**, *21*, 287−291.
18. Ibrahim, A. D.; Entsminger, S. W.; Fout, A. R., Insights into a Chemoselective Cobalt Catalyst for the Hydroboration of Alkenes and Nitriles. *ACS Catal.* **2017**, *7*, 3730−3734.
19. Ben-Daat, H.; Rock, C. L.; Flores, M.; Groy, T. L.; Bowman, A. C.; Trovitch, R. J., Hydroboration of Alkynes and Nitriles Using an α-Diimine Cobalt Hydride Catalyst. *Chem. Commun.* **2017**, *53*, 7333−7336.
20. (a) Chiericato, G.; Arana, C. R.; Casado, C.; Cuadrado, I.; Abruña, H. D., Electrocatalytic Reduction of Carbon Dioxide Mediated by Transition Metal Complexes with Terdentate Ligands Derived from Diacetylpyridine. *Inorg. Chim. Acta* **2000**, *300−302*, 32−42; (b) Pal, R.; Groy, T. L.; Bowman, A. C.; Trovitch, R. J., Preparation and Hydrosilylation Activity of a Molybdenum Carbonyl Complex That Features a Pentadentate Bis(imino)pyridine Ligand. *Inorg. Chem.* **2014**, *53*, 9357−9365.
21. Ghosh, C.; Mukhopadhyay, T. K.; Flores, M.; Groy, T. L.; Trovitch, R. J., A Pentacoordinate Mn(II) Precatalyst That Exhibits Notable Aldehyde and Ketone Hydrosilylation Turnover Frequencies. *Inorg. Chem.* **2015**, *54*, 10398−10406.
22. Small, L. B.; Brookhart, M.; Bennett, A. M. A., Highly Active Iron and Cobalt Catalysts for the Polymerization of Ethylene. *J. Am. Chem. Soc.* **1998**, *120*, 4049-4050.
23. Knijnenburg, Q.; Gambarotta, S.; Budzelaar, P. H. M., Ligand-Centred Reactivity in Diiminepyridine Complexes. *Dalton Trans.* **2006**, 5442−5448.
24. Lu, C. C.; Weyhermüller, T.; Bill, E.; Wieghardt, K., Accessing the Different Redox States of α-Iminopyridines within Cobalt Complexes. *Inorg. Chem.* **2009**, *48*, 6055−6064.
25. (a) Lee, H. K.; Lam, C. H.; Li, S. L.; Zhang, Z. Y.; Mak, T. C., Low-Valent Chemistry of Cobalt Amide. Synthesis and Structural Characterization of Cobalt(II) Amido, Aryloxide, and Thiolate Compounds. *Inorg. Chem.* **2001**, *40*, 4691−4695; (b) Yao, S.; Tam, D. Y. S.; Cheung, P. S.; Lam, C.-K.; Guo, P.; Lam, S. L.; Lee, H. K., Cobalt(II) Amido

Complexes Derived from a Monodentate Arylamido Ligand Featuring a Highly Electron-Withdrawing C_6F_5 Substituent. *Dalton Trans.* **2015**, *44*, 17950−17959.
26. Goodwin, H. A., Spin Crossover in Cobalt(II) Systems. In *Spin Crossover in Transition Metal Compounds II*, Gütlich, P.; Goodwin, H. A., Eds. Springer Berlin Heidelberg: Berlin, Heidelberg, 2004; pp 23−47.
27. Erken, C.; Kaithal, A.; Sen, S.; Weyhermüller, T.; Hölscher, M.; Werlé, C.; Leitner, W., Manganese-Catalyzed Hydroboration of Carbon Dioxide and Other Challenging Carbonyl Groups. *Nat. Commun.* **2018**, *9*, 4521.
28. Suginome, M.; Uehlin, L.; Murakami, M., Aminoboranes as "Compatible" Iminium Ion Generators in Aminative C–C Bond Formations. *J. Am. Chem. Soc.* **2004**, *126*, 13196−13197.
29. The transformations in Table 3 do not require a drying agent and are not sensitive to order of addition; however, we believe that mechanistic similarities may exist between this reaction and boronic acid catalyzed amide coupling. For a recent review see: Hall, D. G. *Chem. Soc. Rev.* **2019**, *48*, 3475-3496.
30. Li, Y.; Li, Z.; Li, F.; Wang, Q.; Tao, F., Preparation of a Nafion-Teflon bimembrane-supported palladium catalyst and its use in the Heck reaction." *Tetrahedron Lett.* **2005**, *46*, 6159-6162.
31. (a) Evans, D. F., The determination of the paramagnetic susceptibility of substances in solution by nuclear magnetic resonance. *J. Chem. Soc.* **1959**, 2003-2005. (b) Schubert, E. M., Utilizing the Evans method with a superconducting NMR spectrometer in the undergradaute laboratory. *J. Chem. Ed.* **1992**, 69, 62.
32. Parr, R. G.; Weitao, Y., *Density-Functional Theory of Atoms and Molecules*. Oxford University Press: 1994; p 352.
33. Bochevarov, A. D.; Harder, E.; Hughes, T. F.; Greenwood, J. R.; Braden, D. A.; Philipp, D. M.; Rinaldo, D.; Halls, M. D.; Zhang, J.; Friesner, R. A., Jaguar: A High-Performance Quantum Chemistry Software Program with Strengths in Life and Materials Sciences. *Int. J. Quantum Chem.* **2013**, *113*, 2110−2142.
34. Zhao, Y.; Truhlar, D. G., The M06 Suite of Density Functionals for Main Group Thermochemistry, Thermochemical Kinetics, Noncovalent Interactions, Excited States, and Transition Elements: Two New Functionals and Systematic Testing of Four M06-Class Functionals and 12 Other Functionals. *Theor. Chem. Acc.* **2008**, *120*, 215−241.
35. (a) Hay, P. J.; Wadt, W. R., Ab Initio Effective Core Potentials for Molecular Calculations. Potentials for the Transition Metal Atoms Sc to Hg. *J. Chem. Phys.* **1985**, *82*, 270−283; (b) Wadt, W. R.; Hay, P. J., Ab Initio Effective Core Potentials for Molecular Calculations. Potentials for Main Group Elements Na to Bi. *J. Chem. Phys.* **1985**, *82*, 284−298; (c) Hay, P. J.; Wadt, W. R., Ab Initio Effective Core Potentials for Molecular Calculations. Potentials for K to Au Including the Outermost Core Orbitals. *J. Chem. Phys.* **1985**, *82*, 299−310.
36. Dunning, T. H., Gaussian Basis Sets for Use in Correlated Molecular Calculations. I. The Atoms Boron through Neon and Hydrogen. *J. Chem. Phys.* **1989**, *90*, 1007−1023.
37. Rashin, A. A.; Honig, B., Reevaluation of the Born Model of Ion Hydration. *J. Phys. Chem.* **1985**, *89*, 5588−5593.

Table of Contents (TOC)